EFSUMB Course Book, 3rd Edition

Editor: Christoph F. Dietrich

Transcranial color-coded duplex ultrasonography of the intracranial vessels

Eva Bartels[1]

[1] Center for Neurological Vascular Diagnostics, München, Germany

Corresponding author

Eva Bartels MD, PhD

Center for Neurological Vascular Diagnostics

Weinstr. 5

80333 München

Email: bartels.eva@t-online.de

On behalf of the European Society of Neurosonology and Cerebral Hemodynamics

www.esnch.org

Introduction

The first attempts to examine intracranial structures through intact bone were made in the 1950s using echoencephalography. The information was obtained from the shift in the midline echo (1, 2). Since then, ultrasonic technology has improved significantly. By the end of the 1970s, two-dimensional B-mode imaging of the brain parenchyma became possible in children through the fontanel (3, 4). In adults, the first B-mode examinations of the brain were initially only possible intraoperatively (5).

At the same time, in 1982, Aaslid introduced transcranial Doppler sonography (TCD), which was widely accepted as a routine method for non-invasive diagnostics of cerebrovascular diseases (6). This method has become extensively used in clinical practice, as it provides valuable information regarding various neurologic conditions, such as subarachnoid hemorrhage and cerebrovascular occlusive disease. It has also been applied for functional testing, emboli detection, in determining circulatory arrest, and other indications (7, 8). Using a pulsed Doppler system with low transmitter frequency, TCD allows blood flow velocities to be recorded from basal cerebral arteries through the intact skull. The intracranial arteries are examined using transtemporal, suboccipital and transorbital approaches. The assignment of the Doppler signals to a specific artery is possible only with the help of indirect parameters: the depth of the sample volume, the position of the transducer, and the direction of the blood flow (9). Therefore, the differentiation of individual vessels with the TCD method can sometimes cause difficulties. The identification of the middle cerebral artery is relatively certain, as it is rarely confused with the neighboring arteries due to its anatomical position.

A lack of orientation points can lead to misjudgments, especially when distinguishing between two arteries with the same flow direction. In the case of unclear anatomical variants and collaterals in the circle of Willis, it may sometimes be necessary to use compression tests. However, compression of the common carotid artery is often associated with methodological problems, and especially in patients with atherosclerotic vascular disease, it can provoke thromboembolic complications. For this reason, compression should not be used (10). Another disadvantage of the conventional TCD method is that it is not possible to visually control the position of the pulsed sample volume in a specific vessel section. In addition, it is not possible to determine the angle of insonation, which leads to inaccurate measurement, especially underestimation of blood flow velocity (11).

The introduction of new, high resolution ultrasound systems and high performance probes has opened up new perspectives for transcranial examinations (12). With the help of the color coding of the Doppler signal, it is not only possible to visualize the blood flow in the intracranial vessels through the intact skull in adults, but also to display their anatomical position and course and to perform exact angle-corrected measurements of the blood flow velocities (13-16). In this chapter, first the examination technique and practical applications of transcranial color-coded duplex sonography (TCCS) are presented. In the second part, the visualization of intracranial cerebral structures and the examination of the brain parenchyma with the B-mode method are described.

Anatomical aspects

Basic knowledge of the intracranial anatomy is mandatory in order to effectively study the use of ultrasound (17) [Figure 1].

Figure 1 **Cerebral arteries (basal view) and circle of Willis. 1 = Superior cerebellar artery; 2 = basilar artery; 3 = pontine branches; 4 = vertebral artery; 5 = anterior spinal artery; 6 = posterior spinal artery; 7 = anterior cerebral artery; 8 = anterior communicating artery; 9 = middle cerebral artery; 10 = internal carotid artery; 11 = posterior communicating artery; 12 = posterior cerebral artery; 13 = artery of labyrinth; 14 = anterior and posterior inferior cerebellar artery; I–VI: cranial nerves. (From Bartels E. Color-Coded Duplex Ultrasonography of the Cerebral Vessels, Atlas and Manual / Farbduplexsonographie der hirnversorgenden**

Gefäße, Atlas und Handbuch. Eurobook bilingual. Stuttgart: Schattauer 2018, p. 50, with permission).

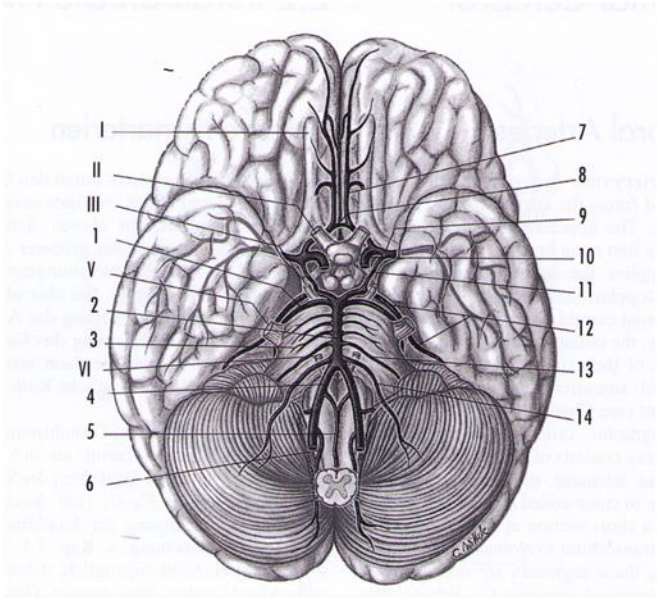

The internal carotid artery runs through the carotid canal to the cranial cavity and forms the curved carotid siphon in the cavernous sinus. The upper region of the carotid siphon is the origin of its first main branch, the ophthalmic artery. The latter supplies the supratrochlear artery, which is important in Doppler ultrasonography. According to angiographic criteria, the intracranial course of the carotid artery consists of six segments (18). The terminal intracranial segment C1 can be visualized well directly before the bifurcation of the internal carotid artery into its main branches, the middle cerebral artery and the anterior cerebral artery. Mostly, the posterior communicating artery which connects the anterior and the posterior circulation joins in the C1 segment. Alternatively, in 10–20% of cases, the posterior cerebral artery arises directly from the anterior circulation. In this so called embryonic origin of the posterior cerebral artery from the internal carotid artery the P1 segment of the posterior cerebral artery is missing or is hypoplastic. The middle cerebral artery has the largest caliber (approx. 3 mm) among the arteries of the circle of Willis and continues laterally of the bifurcation to the hemispheres as the M1 segment. At the Sylvian fissure it divides into 2-5 branches (M2 segment). The anterior cerebral artery runs first medially as the A1 segment and after connecting to the contralateral anterior cerebral artery via the anterior communicating artery

over the optic chiasm, it changes direction rostrally and continues as the A2 segment close to the corpus callosum in the cerebral fissure.

The vertebral artery enters the cranial cavity through the great foramen and runs cephalad between the brain stem and the clivus until it joins with the contralateral vertebral artery to form the unpaired basilar artery. The most important branch of the vertebral artery in its intracranial (V4) segment is the posterior inferior cerebellar artery (PICA), which supplies the dorsolateral medulla oblongata and the cerebellum.

The basilar artery is approx. 3–4 cm long and its course can be straight, curved, or tortuous. The main branches of the basilar artery are the anterior inferior cerebellar artery (AICA) on both sides, superior cerebellar artery on both sides and the terminal branches posterior cerebral artery on the right and left. The basilar artery supplies the basal sections of the temporal and occipital lobes, the cerebellum, the brain stem, and the inner ear. The posterior cerebral artery runs laterally within the ambient cistern (P1 segment) and follows a curved path around the crus of the cerebrum (peduncle of cerebrum) occipitally to the tentorium (P2 segment). Between the P1 and P2 segments the posterior cerebral artery is joined by the posterior communicating artery, which connects the C1 segment of the internal carotid artery to the posterior circulation.

In favorable examination conditions, - especially with a good insonation window – the branches of the main arteries of the circle of Willis, and the C2-C6 segments of the internal carotid artery can also be visualized (18).

Examination Technique

The transcranial sonography requires the use of lower frequency sector transducers to adequately penetrate the skull to produce useful B-mode images and to record Doppler signals. A 1.6 - to 3.5-MHz transducer or multifrequency transducer with 2- to 3- MHz spectral capability is commonly used (17, 19, 20). The patient is examined in the supine position, with the head in the midline. The examiner sits behind the patient`s head. Both the examiner and the patient must be comfortable because, particularly in pathological conditions, the evaluation may take a long time (more than 20-30 minutes).

Transtemporal Examination

The routine transtemporal examination is carried out in the axial plane. This level corresponds to the axial plane of the magnetic resonance imaging through the orbitomeatal line and enables the visualization of the middle cerebral artery, anterior cerebral artery and posterior cerebral artery [Figure 2].

Figure 2 **Examination technique for intracranial vessels. Schematic image of the sectional planes for transtemporal (left), suboccipital (center), and transorbital insonation (right) (From Bartels E. Color-Coded Duplex Ultrasonography of the Cerebral Vessels, Atlas and Manual / Farbduplexsonographie der hirnversorgenden Gefäße, Atlas und Handbuch. Eurobook bilingual. Stuttgart: Schattauer 2018, p. 217, with permission).**

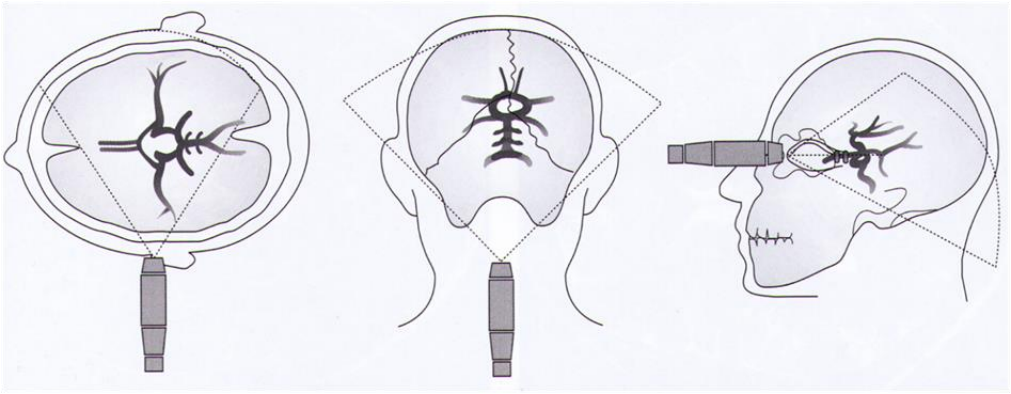

The examination begins in B mode with an examination depth of initially 14-16 cm. To ensure that images generated from the right and from the left are anatomically comparable, the transducer is always placed with the marker to the front. Usually, anterior sections of the brain are shown in the image on the left. Using the transtemporal approach the transducer is placed at the temporal bone above the zygomatic arch and anterior to the ear. Imaging of the basal cerebral arteries with transtemporal insonation is shown in Figures 3 - 6.

Figure 3 **Magnetic resonance image of the anatomical position of the arteries of the circle of Willis in the same plane as in Figure 4.**

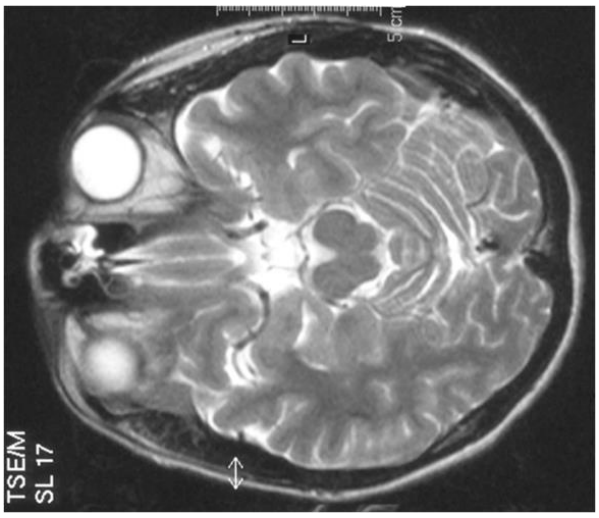

Figure 4 **Schematic view in the axial plane with transtemporal insonation of the basal cerebral arteries in the same plane as in [Figure 3] (Figure 4 from Bartels E. Color-Coded Duplex Ultrasonography of the Cerebral Vessels, Atlas and Manual / Farbduplexsonographie der hirnversorgenden Gefäße, Atlas und Handbuch. Eurobook bilingual. Stuttgart: Schattauer 2018, p. 222, with permission).**

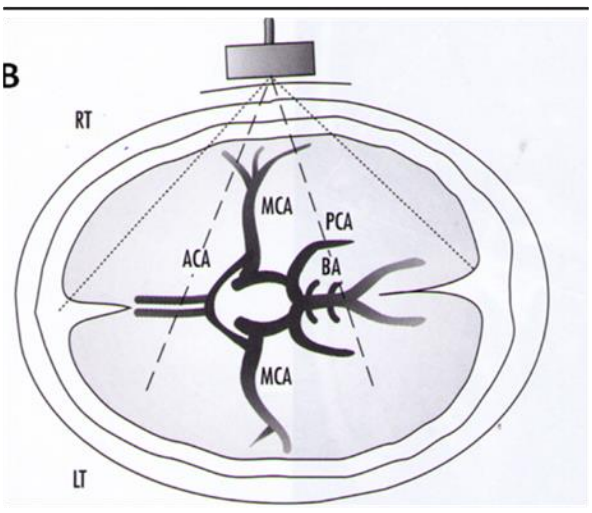

Figure 5 **B-mode image of the brain parenchyma in the axial mesencephalic plane with transtemporal insonation. *= brainstem, yellow arrows = gyri of the cerebellum, black arrows = contralateral skull. Examination depth =140 mm.**

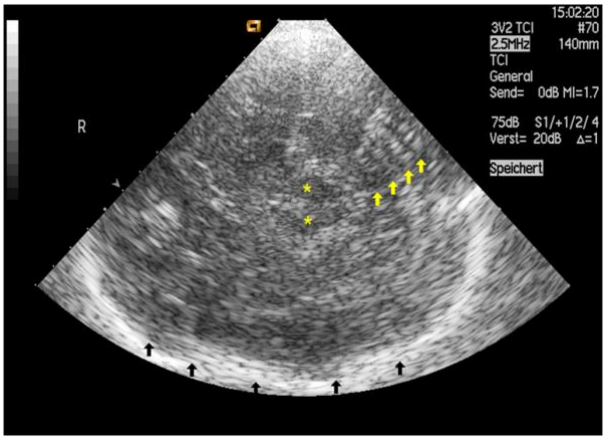

Figure 6 **Color-coded duplex sonography of arteries of the circle of Willis. Angle-corrected Doppler spectrum of the middle cerebral artery (insonation angle = 21°). The middle cerebral artery = MCA (1), the posterior communicating artery (2), the A1 segment of the ipsilateral anterior cerebral artery = ACA (3), the A1 segment of the contralateral ACA (4), the A2 segment of the ipsi- and contralateral ACA (5), the contralateral MCA (6), the P1 segment of the ipsilateral posterior cerebral artery = PCA (7) and the P1 segment of the contralateral PCA (8). *= mesencephalic brain stem, yellow arrows= contralateral skull.**

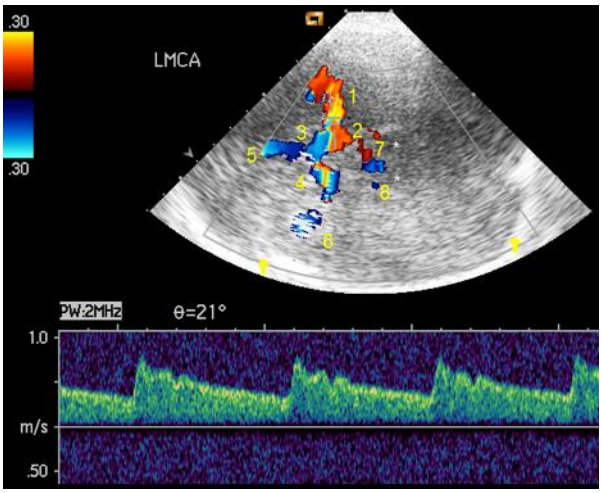

In this transducer position the hypoechoic butterfly-shaped cerebral peduncles, surrounded by the hyperechoic neighboring cisterns can be imaged in the axial plane on gray-scale B-mode image. By slightly angling the transducer apically (about 10°) in the diencephalic plane, the thalamus, the third ventricle in the middle and the pineal gland appear. In order to scan axial sections in the plane through the cella media the transducer is tilted further cranially (by 30°) (21, 22). By turning the transducer from the axial plane by 90° the coronal plane can be displayed. Further details concerning B-mode brain parenchymal imaging are described in the next chapter.

After optimizing the probe position using the described B-mode structures, the color Doppler mode is selected. The individual arteries can be identified on the basis of their anatomical position with respect to the brain stem structures and on flow directions. The lesser sphenoid wing serves as a B-mode landmark for the terminal internal carotid artery and the siphon (23). Vessels with flow towards the transducer are coded red while those with flow away from the transducer are coded blue (24). Accordingly, assuming normal flow conditions, the transtemporal insonation displays the ipsilateral middle cerebral artery (MCA) in red and the two segments (A1 and A2) of the ipsilateral anterior cerebral artery (ACA) are imaged in blue. Usually a long M1 segment of the MCA can be visualized because its proximal part runs in the axial plane. In elderly patients it can be recognized on B-mode image as a hyperechoic pulsatile structure located parallel to the lesser wing of the sphenoid bone. By using the color function of the device, the trifurcation and the larger branches can be visualized. It is often possible to simultaneously image the contralateral MCA (coded blue since the direction of flow is away from the transducer). Accordingly, the A1 segment of the contralateral ACA is coded red. The evaluation of the flow direction in the anterior cerebral artery is important for the assessment of the collateral circulation in cerebral occlusive disease (25, 26).

By slightly angling the transducer caudally, the terminal C1 segment of the internal carotid artery (coded red) – usually displayed in diagonal plane – is visible. In the anterior coronal plane the course of the internal carotid artery can easily be followed in the carotid sulcus to its bifurcation into ACA and MCA. The carotid siphon can be visualized using the combined transtemporal axial / coronal approach (27).

The posterior cerebral artery (PCA) winds posteriorly and laterally around the brainstem. It is not always possible to visualize it in the same plane as the MCA and the ACA. The transducer

must be slightly tilted occipitally. Because of its curved course, usually the precommunicating P1 segment and the proximal (anterior) portion of the postcommunicating P2 segment of the PCA, with flow towards the transducer, are coded red, and the distal (posterior) P2 segment, with flow away from the transducer, is coded blue.

The posterior P2 segment and the basal vein of Rosenthal can sometimes be imaged simultaneously in the diencephalic plane since they run relatively close to each other. The Doppler signal then exhibits a mixed signal of the artery and the vein (28, 29). By turning the transducer 90° at the level of the P1 segment of the PCA, the top of the basilar artery can be visualized in the posterior coronal plane.

Transnuchal Examination

The examination is carried out with the same device technology as with the temporal access. Transnuchal (suboccipital) sonography can be performed on the patient in a sitting or lying lateral position, with the head slightly tilted forward. The examination starts in B mode with an examination depth of 10-12 cm. The key structure for identifying the vessels is the great foramen, which appears as a hypoechoic circular area with a hyperechoic boundary at a depth of 4.5-6.5 cm. The transducer is moved until the great foramen can be displayed in the center of the image as far as possible. Imaging of the basal cerebral arteries with suboccipital insonation is shown in Figures 7-9.

Figure 7 **Schematic view of the sectional plane with suboccipital insonation of the terminal segments of the vertebral arteries and the basilar artery.**

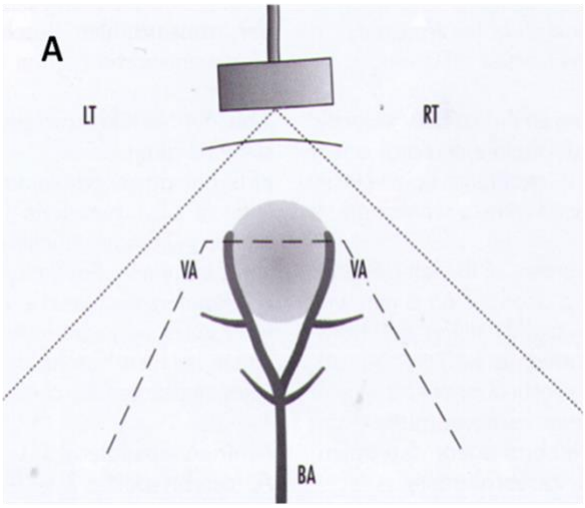

Figure 8 **Transducer position for suboccipital (transforaminal) insonation. (Figure 7, 8 from Bartels E. Color-Coded Duplex Ultrasonography of the Cerebral Vessels, Atlas and Manual / Farbduplexsonographie der hirnversorgenden Gefäße, Atlas und Handbuch. Eurobook bilingual. Stuttgart: Schattauer 2018, pp. 217 and 225).**

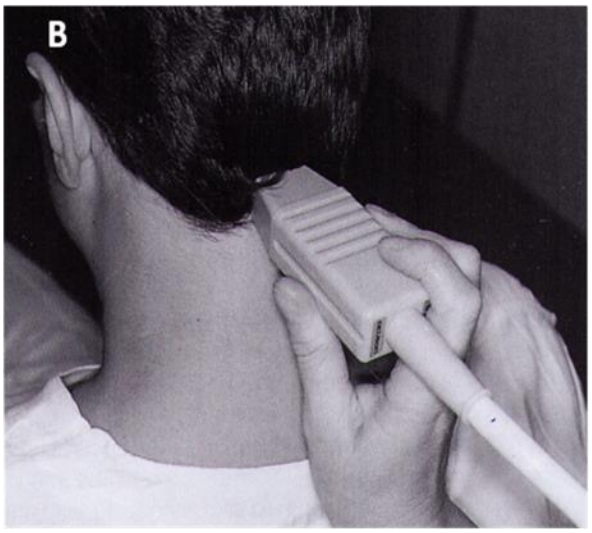

Figure 9 **Visualization of both vertebral arteries and the basilar artery by insonating through the great foramen, corresponding to the scheme shown in [Figure 7]. The basilar artery and the cranial segments of the vertebral arteries are coded blue, with flow away from the transducer. 1= basilar artery, 2= vertebral artery. In their proximal V4 segment, both vertebral arteries are coded red (2a) - caused by their tortuous course in the great foramen region (*).**

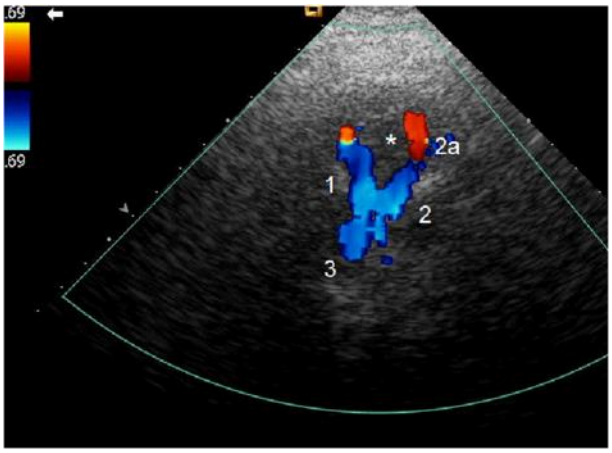

The transnuchal insonation is used for the examination of the proximal portion of the basilar artery (BA) and the intracranial (V4) segment of the vertebral arteries (VA) (30, 31). After switching to the color mode the two vertebral arteries can be easily recognized lateral in the great foramen. Normal flow in the vertebral artery and in the basilar artery is shown in the direction away from the transducer, coded blue. (32). The confluence of the vertebral arteries to form the basilar artery can be shown at variable depths, usually around 70-80 mm. While the visualization of the vertebral artery and the initial section of the basilar artery are possible in most cases, the visualization of branches of the vertebral artery and basilar artery is not always successful. The posterior inferior cerebellar artery is most likely to be imaged. It branches off from the V4 segment of the vertebral artery and can be usually imaged well with red color-coding due to the flow towards the transducer.

Intracranial vascular diagnostics via the transnuchal access is more difficult because of the often tortuous course of the vessels. Under optimal examination conditions it is sometimes possible to visualize the "Y" configuration of the converging vessels.

A Doppler spectrum with angle correction should be recorded from the vertebral artery on both sides and from the basilar artery. As mentioned above, a statement about the top of the basilar artery is possible by transtemporal examination of its terminal branches (arteria cerebri posterior).

Transorbital Examination

Transorbital insonation allows visualization of the ophthalmic artery and the carotid siphon (33-35), [Figure 2]. It is important during transorbital examination that the acoustic energy is reduced to a maximum of 10%–15% in order to prevent possible ocular injury.

Hemodynamic Parameters

To record the Doppler spectrum, the sample volume is placed under visual control in the vessel segment of interest – if possible, over a long stretch of the vessel, at least 1.0-1.5 cm long (36). The Doppler spectrum should always be displayed, not only to enable the identification of the vessel, but also to measure the hemodynamic parameters – systolic and end diastolic flow velocities, pulsatility index, and to detect possible side to side differences. The Doppler spectrum of the intracranial arteries is characterized by a high diastolic component (17). To obtain a more exact measurement of flow velocity, angle correction is carried out by manually positioning the cursor of the sample volume as parallel as possible to the vessel wall.

Whilst with conventional pulsed Doppler sonography (TCD) flow velocity can only be determined in a small, defined sample volume, color-coded duplex sonography enables blood flow in an entire vessel section to be visualized in real time. After angle correction the measured flow velocity values are 3-30% higher (depending on the examined vessel) in comparison with the values measured with the conventional transcranial Doppler sonography, where the insonation angle is not considered at all (37).

The normal values for the maximum systolic and mean flow velocities of the intracranial arteries exhibit a wider scatter than those of the extracranial carotid artery and they differ from study to study (38, 39). This is primarily due to the use of different technical equipments, and by different anatomical conditions. The normal values for mean flow velocities in the different cerebral arteries are presented in Table 1.

Table 1 Mean values of systolic and enddiastolic blood flow velocities (BFV) in basal cerebral arteries (39)

	Systolic BFV (cm/s)	Enddiastolic BFV (cm/s)
MCA	110 (100-119)	50 (40-55)
ACA	95 (80-105)	40 (30-50)
PCA	70 (55-75)	35 (20-30)
VA	55 (40-60)	25 (20-30)
BA	60 (50-70)	35 (30-35)

Flow velocities are higher in women than in men, and decrease with age, whereas pulsatility increases with age (40).

In summary, using the color-coded procedure, the following information may be obtained simultaneously:

- Vessel identification and anatomical position.
- Information on the time course of the flow parameters (spectrum analysis).
- Information on the spatial distribution of the flow velocities, on the flow direction, and flow disturbances.

Pathological findings. Clinical aspects

Despite the technical difficulties at the beginning of the transcranial duplex ultrasonography period, during the last three decades TCCS found its important role in the routine diagnostics of cerebrovascular diseases.

In the second part of this chapter an overview of the possible indications for TCCS in the clinical routine in the examination of the intracranial arteries will be presented. Transcranial sonography of the cerebral parenchyma is described in the next chapter.

Stenoses of the cerebral arteries

The degree of stenosis of an intracranial artery is estimated on the basis of the changes of the Doppler spectrum (increased flow velocities in the area of the stenosis, and flow disturbances upstream and downstream from the lesion). It is relatively easy to detect a stenosis in the proximal segment of the middle cerebral artery. The thickened vessel wall in the area of the stenosis can be imaged even in B-mode due to its higher echogenicity (41). Example of a high-grade stenosis of the left middle cerebral artery and the basilar artery in a 76-year-old patient with multiple vascular risk factors (hypercholesterolemia, hypertension, nicotine abuse) is shown in Figures 10 - 13.

Figure 10 **Visualization of a stenosis in the middle cerebral artery on the left at a depth of 62 mm (yellow arrows). The aliasing phenomenon, also visible when the color scale is increased to mean flow velocity of 69 cm/s (red arrows), indicates a higher-grade stenosis. The Doppler spectrum shows an increased maximum systolic flow velocity (257 cm/s) with flow disturbances and a filled in systolic window (white arrows). *= brainstem.**

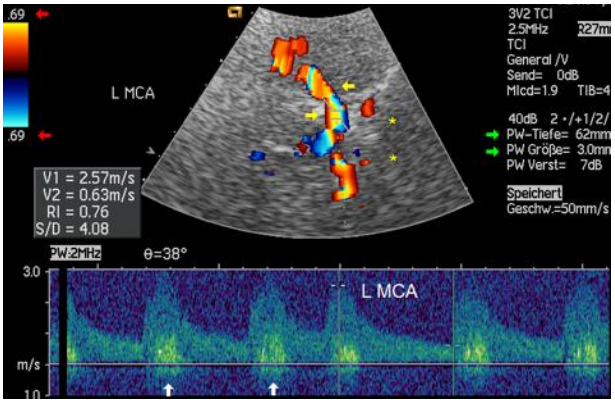

Figure 11 **High grade stenosis at the junction of the right vertebral artery and the basilar artery. Aliasing phenomenon as an indication of a significantly increased blood flow velocity. Maximum systolic flow velocity at a depth of 79 mm is 253 cm/s,**

(white arrow = position of the sample volume, yellow arrow =insonation angle of 11°).

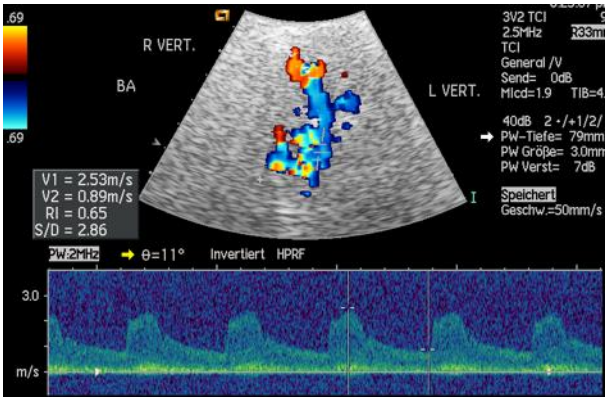

Figure 12 **The Doppler spectrum of the right vertebral artery recorded at a depth of 56 mm (white arrow) shows increased pulsatility proximal to the high-grade stenosis. (Maximum systolic flow velocity = 88 cm/s, yellow arrow = insonation angle of 10°).**

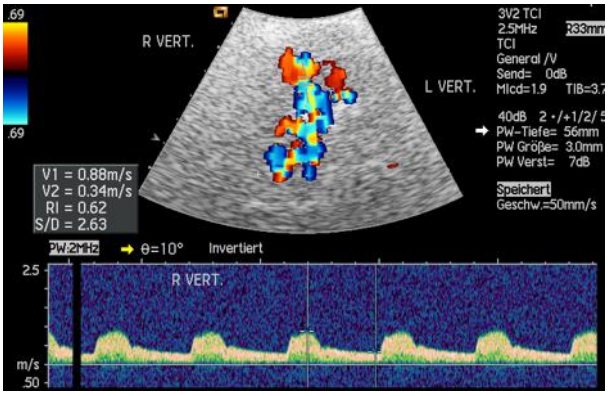

Figure 13 **MR angiographic image of the high-grade stenosis of the middle cerebral artery on the left (arrow) and the right vertebral artery at the transition to the basilar**

artery (double arrow). (Diagnostic and Interventional Neuroradiology, University Medicine Göttingen).

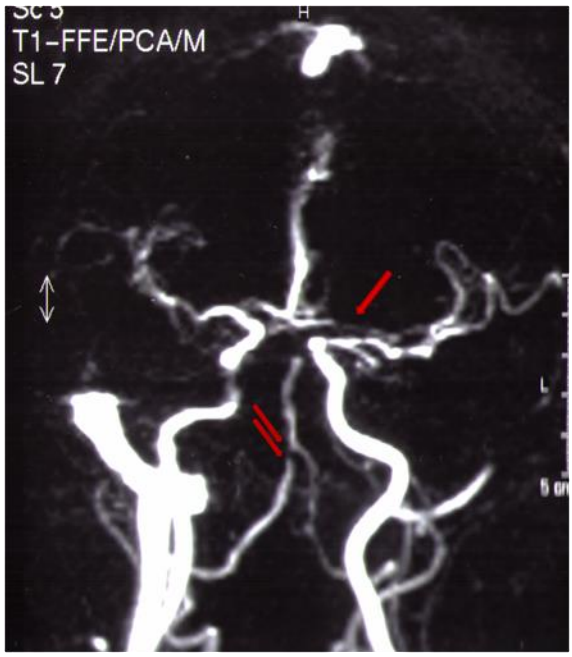

Compared to that, direct color-coded duplex sonography imaging of an intracranial stenosis of the internal carotid artery (e.g. in the region of the carotid siphon) is more difficult. Such a diagnosis is made on the basis of indirect extracranial findings which indicate a distal obstruction to flow (42). Intracranial stenoses occur relatively seldom in the anterior and posterior cerebral artery. On the other hand, the distal intracranial vertebral artery (in V4 segment) and the basilar artery are preferred sites for atherosclerotic intracranial stenoses (43). It is difficult to precisely quantify intracranial stenoses by sonography because appropriate angiographic standards are lacking. Several diagnostic criteria have been developed to identify hemodynamically significant stenosis in various intracranial arteries, for both transcranial Doppler (TCD) and transcranial color-coded sonography. However, none of these criteria is absolute. Consequently it is important to validate these velocity values in each neurosonological laboratory against angiographic findings (44). The main goal of transcranial ultrasound in patients with ischemic stroke is to detect a hemodynamically significant stenosis equal or higher than 50% [Table 2] (45).

Table 2 TCCS criteria for intracranial stenosis (45).

	Mild stenosis </=50%	Moderate stenosis >/=50%
	Peak systolic velocity	Peak systolic velocity
MCA	>/= 155 cm/s	>/= 220 cm/s
ACA	>/= 120 cm/s	>/= 155 cm/s
PCA	>/= 100 cm/s	>/= 145 cm/s
VA	>/= 100 cm/s	>/= 140 cm/s
BA	>/= 90 cm/s	>/= 120 cm/s

Vasospasms of the cerebral arteries

Differentiation between a stenosis and a vasopasm can sometimes be difficult. In the case of a stenosis the aliasing phenomenon is usually visible in a circumscribed, short section of the vessel, corresponding to the stenotic segment, whereas, with a vasospasm several vessels are often affected. Color-coded duplex sonographic images of vasospasms involving several are usually affected at the same time. This is shown by increased flow velocities, which are recognized by the aliasing phenomenon. Color-coded duplex sonographic images of vasospasms involving several basal cerebral arteries and the change of the color coding by adjusting the scale (PRF) are shown in figures 14-17.

Figure 14 **If several basal cerebral arteries are involved, the aliasing phenomenon can be seen in all visualized vessels. Arrows = adjustment of the color scale to 30 cm/s mean flow velocity.**

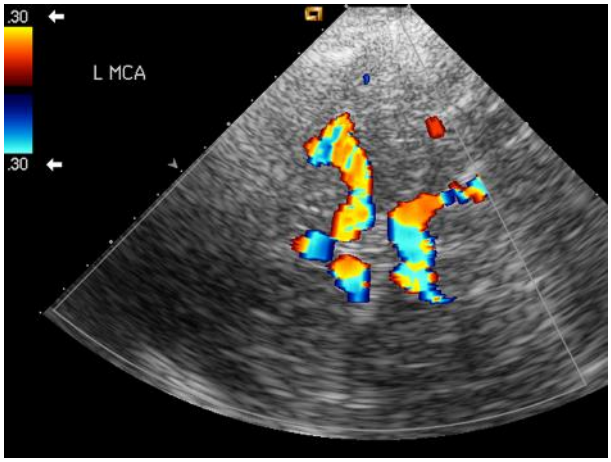

Figure 15 **By gradually increasing the color scale from 40 cm/s to 60 cm/s (arrows), the individual arteries of the circle of Willis can be clearly identified based on the flow direction using the color coding. The aliasing phenomenon is less noticeable.**

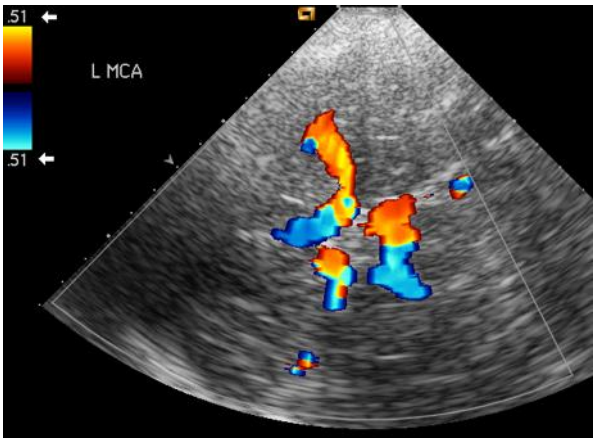

Figure 16 **Increased flow velocities can be documented in the Doppler spectrum from the individual vessel segments under visual control. The color scale is set to 30 cm/s mean flow velocity, therefore, the aliasing phenomenon can be seen in all**

visualized vessels.The maximum systolic flow velocity in the middle cerebral artery = 180 cm/s indicates a significant vasospasm (according to Widder 1999). Angle of insonation = 54°.

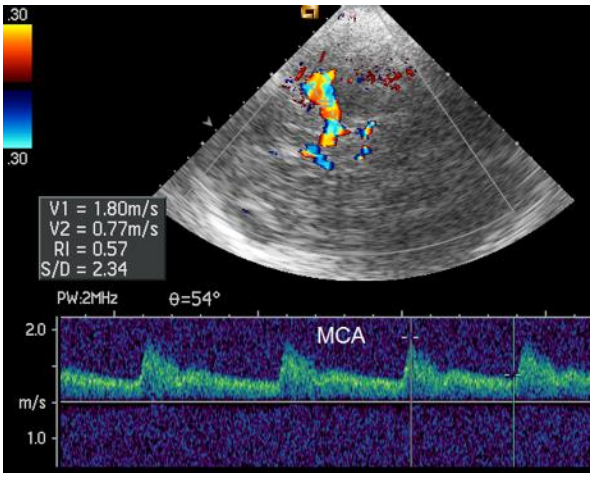

Figure 17 **Evidence of increased flow velocities in the posterior circulation with suboccipital insonation. The maximum systolic flow velocity in the basilar artery of 106 cm/s is in the upper normal range, which in this case does not indicate a vasospasm. Angle of insonation = 13°.**

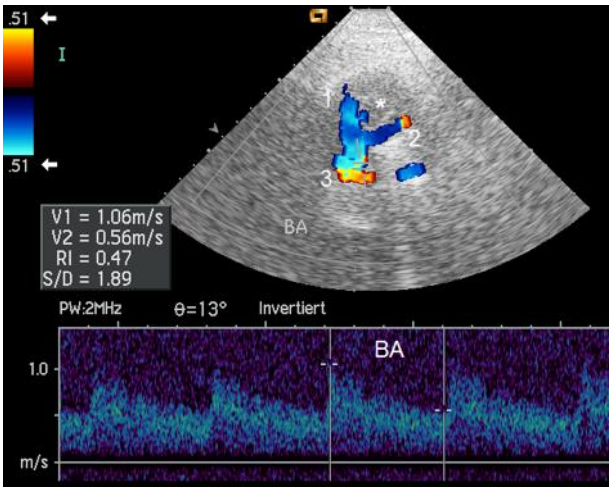

Intracranial collateral pathways

Increased flow velocities can also be recorded due to the compensatory increase in blood flow through **collateral vessels** in the case of obstructive lesions in the contralateral hemisphere, in extracranial carotid disease or in flow obstruction in vertebrobasilar circulation. The proper functioning of the circle of Willis is important for the collateral supply of an underperfused region. Images of an occlusion of the internal carotid artery at the origin with good intracranial collateralization are shown in figures 18-21.

Figure 18 **View of an occlusion of the right internal carotid artery at the origin. The lumen of the internal carotid artery is completely filled in with homogeneous material. The arrows indicate the border to the open lumen of the common carotid artery which is displayed by red color coding. The Doppler spectrum was taken proximal to occlusion. The missing diastolic portion of the Doppler spectrum suggests a distal flow obstruction (arrows).**

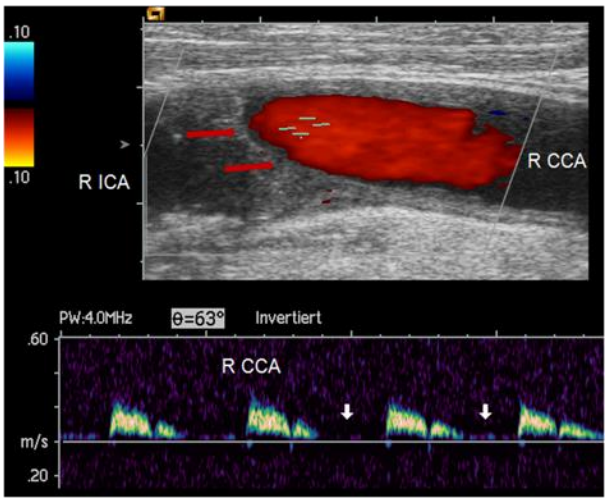

Figure 19 **Transcranial image of the circle of Willis with insonation from the left temporal side. The aliasing phenomenon in all visualized vessels indicates an increased flow velocity due to good collateralization of the right hemisphere via the anterior and posterior communicating arteries. 1= left middle cerebral artery, 2= left anterior cerebral artery (A1 segment), 3= right anterior cerebral artery (A1**

segment), 4= anterior cerebral artery (A2 segment – right and left), 5=right middle cerebral artery, 6=right posterior communicating artery, 7=left posterior communicating artery, 8=left posterior cerebral artery (P1 segment), 9= left posterior cerebral artery (P2 segment). *= brainstem.

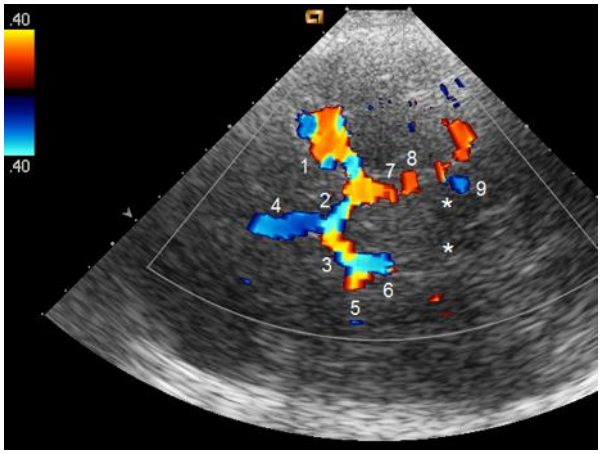

Figure 20 **MRA showing the occlusion of the right internal carotid artery at the origin (arrow).**

Figure 21 There is no signal from the internal carotid artery in the siphon area (arrows). (Radiology Dr. Sollfrank, Munich).

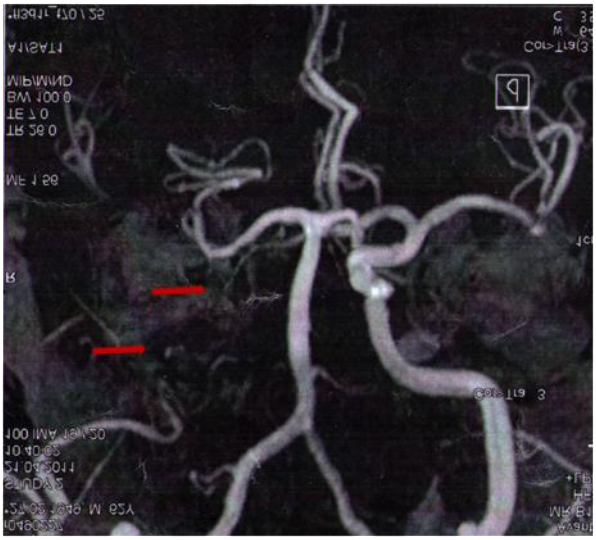

In the circle of Willis the anterior and posterior circulatory systems are connected by the posterior communicating arteries and the right and left carotid systems are connected by the anterior communicating artery. The circle of Willis is complete only in 20% of cases (46, 47). Most often numerous variations are observed in which one or several vascular segments may be hypoplastic or aplastic. Images of intracranial collateral pathways with an insufficient anterior collateralization and a good vertebrobasilar collateralization in a 75-year-old patient with left arm hemiparesis as a result of cerebral ischemia 15 years ago due to occlusion of the right internal carotid artery are shown in figures 22 - 27.

Figure 22 Color-coded image of the right carotid bifurcation. The lumen of the internal carotid artery is filled in with echogenic material. At the origin of the internal carotid artery (2 arrows in the image), only pulsation artefacts caused by the

occlusion can be recorded with the Doppler sonography (arrows in the Doppler spectrum).

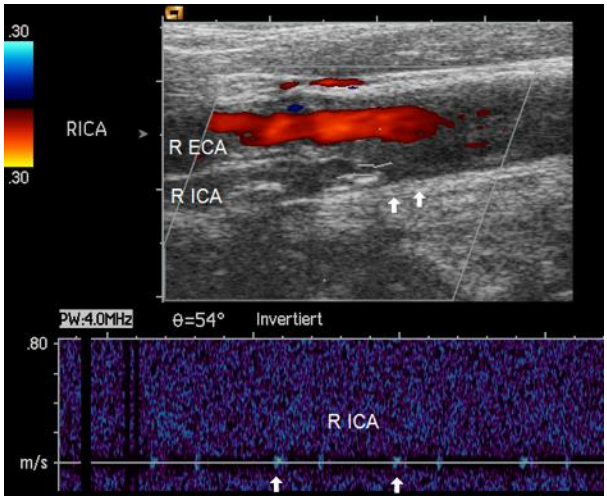

Figure 23 **Transcranial findings in the anterior circulation using transtemporal insonation on the right show poor collateral supply with the absence of the right anterior cerebral artery (arrow). The sample volume of the Doppler spectrum is located in the left middle cerebral artery. 1 = Right posterior cerebral artery, 2 = Left posterior cerebral artery, 3 = Right middle cerebral artery, 4 = Left middle cerebral artery, 5 = Anterior communicating artery.**

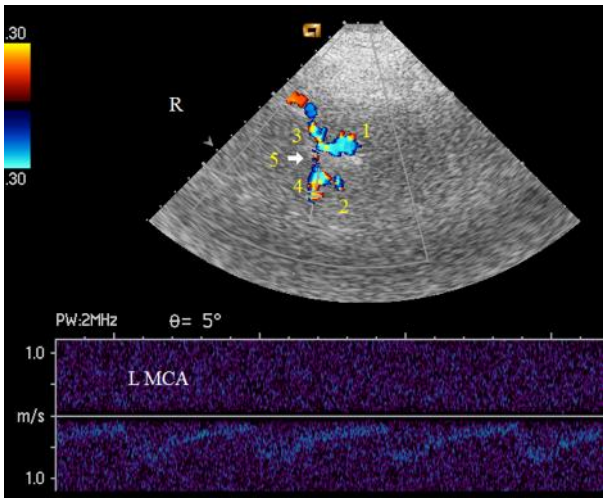

Figure 24 **Strong flow in the intracranial segments of the vertebral arteries (1, 2) as well as in the basilar artery (3) indicates a good vertebrobasilar collateral supply. Maximum systolic flow velocity in the basilar artery = 78cm/s.**

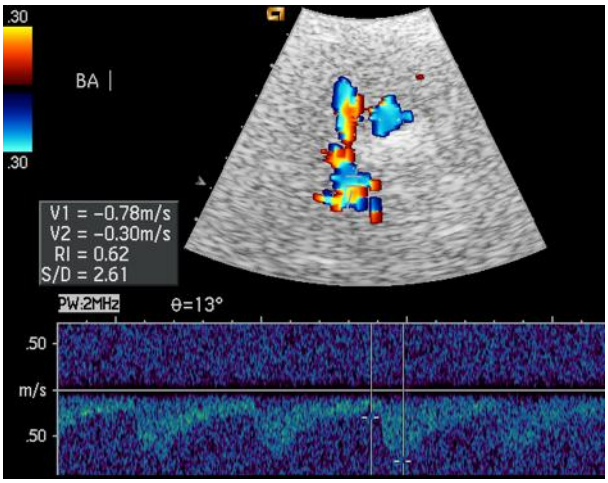

Figure 25 **MR angiography of the extracranial arteries supplying the brain shows an occlusion of the right internal carotid artery from its origin and a mild longitudinal stenosis of the external carotid artery at its origin (arrow). (Radiology Dr. Sollfrank, Munich).**

Figure 26 **MR angiography of the intracranial arteries supplying the brain showing a normal right middle cerebral artery with supply from the posterior circulation via the relatively strong right posterior communicating artery. There is also an occlusion of the A1 segment of the right anterior cerebral artery (arrow) (Radiology Dr. Sollfrank, Munich).**

Figure 27 **MRI of the neurocranium shows an extensive right temporal cortical/subcortical substance defect extending to the Sylvian fissure and medially to the lateral basal ganglia (arrows). Findings compatible with the past ischemic cerebral**

infarction in the territory of the right middle cerebral artery (Radiology Dr. Sollfrank, Munich).

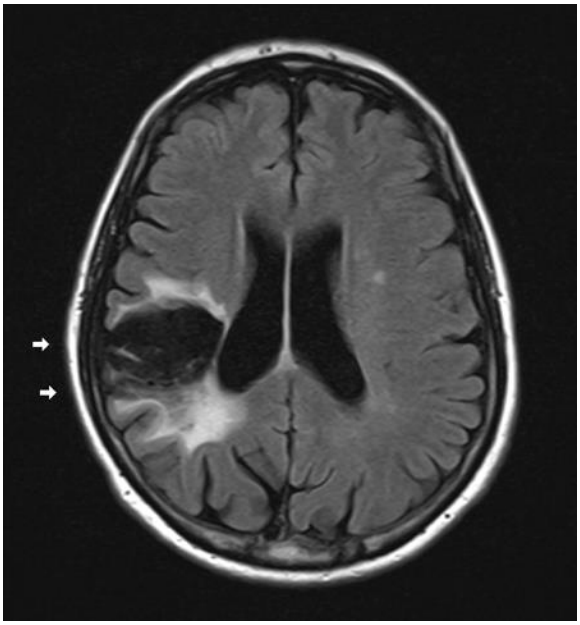

The presence of collateral pathways allows a prognosis to be made in the case of an acute vessel obstruction (48, 49). The examiner should, however, be familiar with extracranial findings, in order to avoid misinterpretation.

Occlusions of the cerebral arteries

Of particular clinical relevance is an occlusion of the middle cerebral artery. It can arise due to a local thrombosis in an atherosclerotic lesion, or occasionally in vasculitis, moyamoya disease, or coagulopathy. Most often, however, it is caused by embolism due to either cardiac or arterial sources for the emboli. An early diagnosis in patients with cerebral ischemia is crucial for the therapeutic strategy, especially in the decision for a thrombolysis (23).

Sonographic diagnosis of occlusion of a cerebral artery can be made when a color-coded signal cannot be obtained at the depths of insonation corresponding to that artery, although neighboring arteries can be imaged well [Figures 44-47]. Criteria for the sonographic diagnosis of the occlusion of the middle cerebral artery in the axial plane include lack of detectable flow in the middle cerebral artery, good visualization of the ipsilateral posterior cerebral artery, and detection of the collateral flow (17).

Intracranial arteriovenous angioma

The sonographic detection of arteriovenous malformations is based on direct and indirect diagnostic criteria. The color-coded image is very characteristic: an arteriovenous malformation consists of convolutes of vascular loops with different flow directions and increased flow velocities in the angiomatous vessels which cause aliasing phenomena (50). Color-coded duplex ultrasonographic images of an extensive arteriovenous malformation located bilaterally in the basal brain region in a 64-year-old patient with epileptic seizures are shown in figures 28 - 30.

Figure 28 Multicolored signals due to the aliasing phenomenon, which corresponds to the vascular convolutes of the malformation and can be recognized immediately.

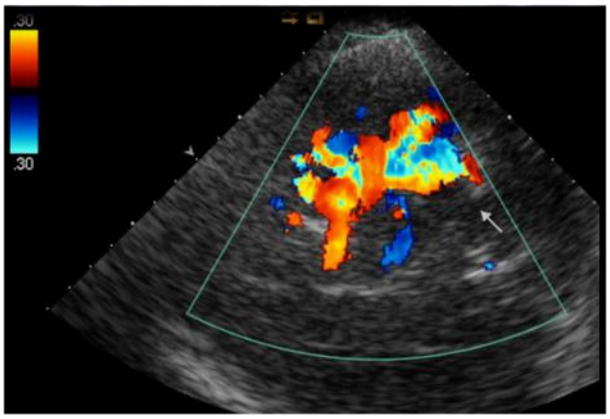

Figure 29 Typical Doppler spectrum of the arteriovenous malformation. An AVM is characterized by low pulsatility of the Doppler spectrum with increased diastolic flow velocity due to the low peripheral resistance (resistance index < 0.45).

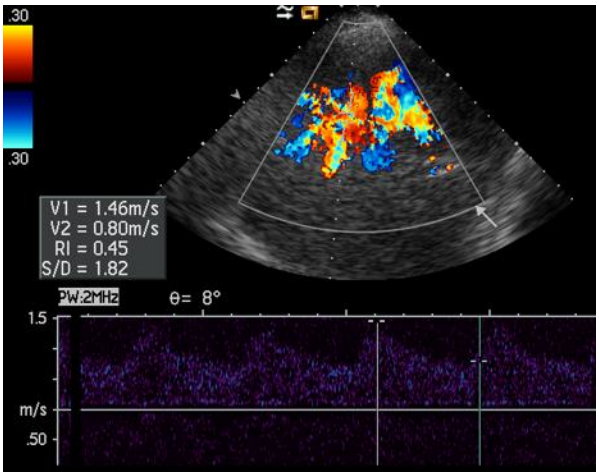

Figure 30 Computed tomographic image of the arteriovenous malformation in the axial examination plane.

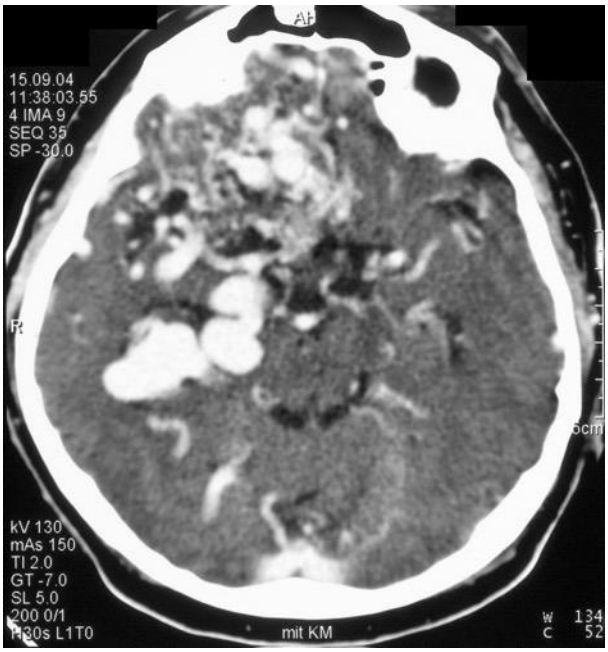

Indirect criteria are increased systolic and diastolic flow velocities with reduced pulsatility of the Doppler spectrum in the feeding arteries. With these criteria, most malformations with a diameter > 2 cm can be identified if they are in a suitable examining plane.The axial imaging plane offers the greatest advantages in visualization. Sonographic assessment of malformations which are located outside this sonographic imaging plane, mainly subcortical,

is limited. These can be sometimes indirectly detected by identifying feeder arteries and draining veins (51). For this reason, sonography should not be used for screening of AVM. On the other hand, as a noninvasive method this technique is suitable for postoperative follow-up. After surgical therapy or after embolization, a reduction in the vascular convolutes and a normalization of the hemodynamic parameters can be observed.

Intracranial aneurysms

An aneurysm is imaged as a color-coded appendix with a round or oval structure next to a normal vessel. Depending on the size it shows an inflow and outflow zone with opposite flow and correspondingly different color coding in the color mode (52, 53). Due to the spatial resolution, aneurysms with a diameter of less than 5 mm are often undetected. In a favourable location even these small aneurysms can be imaged, but then mostly without a flow reversal. Intracranial aneurysm is shown in figures 31 - 34. Incidental finding of a saccular aneurysm of the right internal carotid artery in a 38-year-old man. 1 = right middle cerebral artery, 2 = terminal C1 segment of the right internal carotid artery, 3 = terminal C1 segment of the left internal carotid artery, 4= left middle cerebral artery. Arrow = aneurysm.

Figure 31 Color-coded duplex ultrasonographic visualization of an aneurysm at the transition of the terminal right internal carotid artery into the middle cerebral artery using transtemporal insonation on the right in the coronal plane (arrow). The aneurysm is shown coded blue.

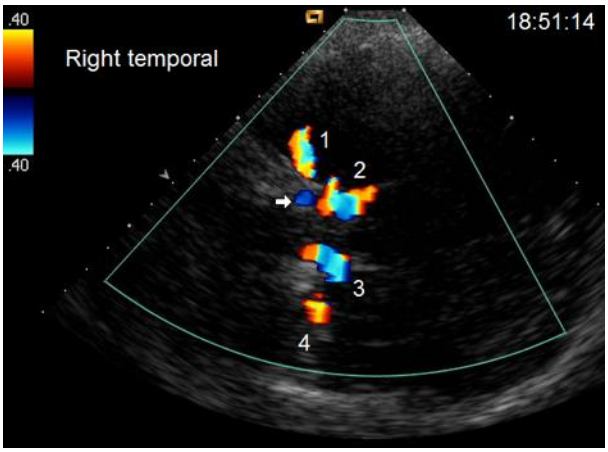

Figure 32 **A typical finding of a flow reversal within an aneurysm (see text) cannot be shown due to the small diameter of approx. 3 mm. In this case, the flow disturbances within the aneurysm can only be identified using the Doppler spectrum.**

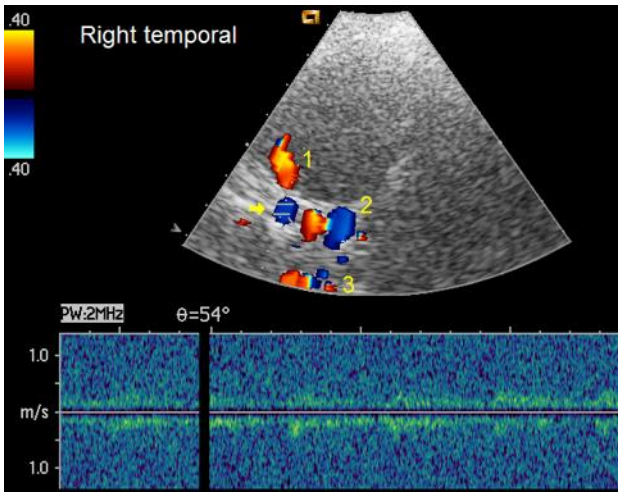

Figure 33 **The Doppler spectrum of the right middle cerebral artery is regular. 1 = right middle cerebral artery, 2 = terminal C1 segment of the right internal carotid artery, 3 = terminal C1 segment of the left internal carotid artery, 4= left middle cerebral artery.**

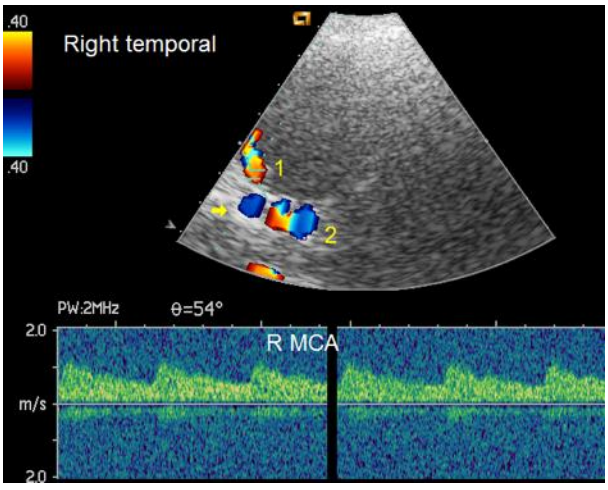

Figure 34 MR angiography showing the 3 mm saccular aneurysm of the right internal carotid artery in the terminal segment (arrow). Otherwise unremarkable MR angiography findings. (Radiology Dr. Sollfrank, Munich).

Furthermore, the detection of partially thrombosed aneurysms and more peripherally located aneurysms is severely limited. Therefore, the method is not suitable as a screening method for intracerebral aneurysms. Color-coded duplex sonography is advantageous for non-invasive follow-up studies after endovascular aneurysm treatment and for postoperative monitoring.

Contrast agents

The domain of transcranial color-coded duplex sonography is the imaging of the arteries supplying the brain. The insonation through the intact skull through an appropriate transtemporal bone window and the associated sound absorption and scattering is the main obstacle of the investigation. Contrast-enhanced ultrasound transcranial color-coded duplex sonography (CE-TCCS) significantly improves the imaging quality and the validity of the examination (54). Imaging of the intracranial arteries with contrast-enhanced transcranial color-coded duplex sonography (CE-TCCS) is shown in Figures 35 - 38. The intracranial vessels can be better visualized with the help of an echo contrast agent, if the bone window is insufficient [Figures 35 - 38].

Figure 35 **Transtemporal examination of the circle of Willis before administration of a contrast agent.**

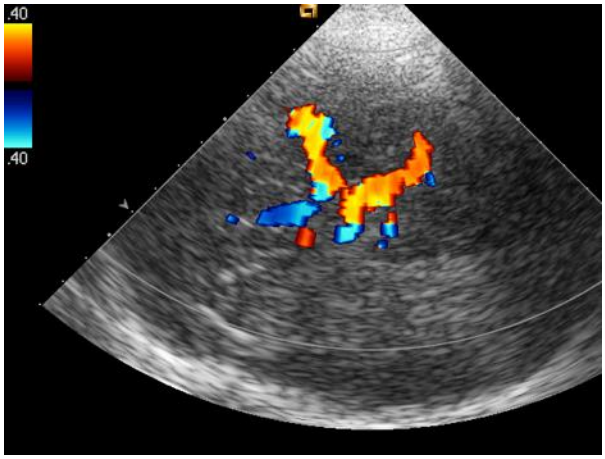

Figure 36 **After the application of the contrast agent, a so-called "blooming artifact" appears with intensified color-coded signals.**

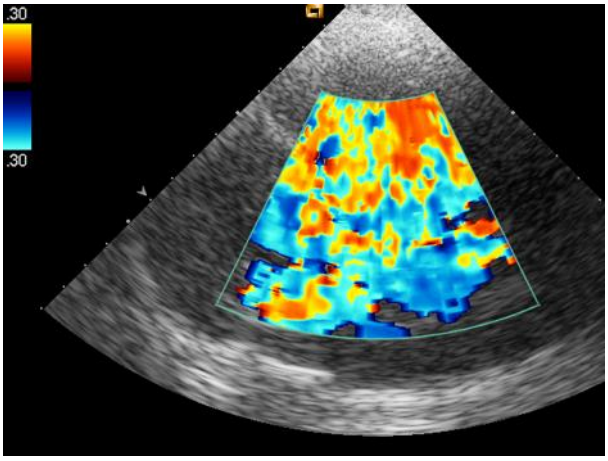

Figure 37 After waiting a few heart cycles, the singular arteries of the circle of Willis can be clearly visualized and easily identified based on the flow direction.

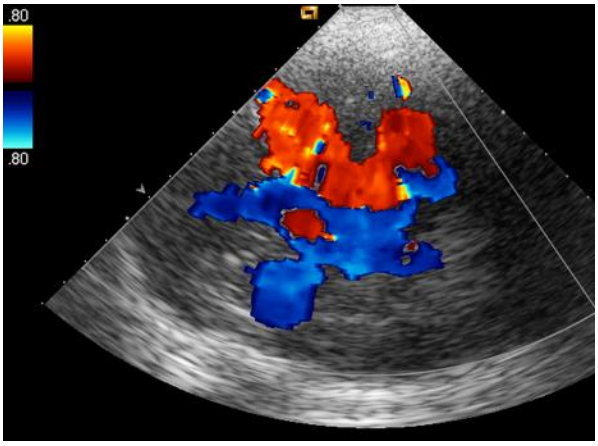

Figure 38 For better differentiation of the contrast-enhanced signal, the color scale (PRF) is set in the upper measuring range (80 cm/s mean flow velocity).

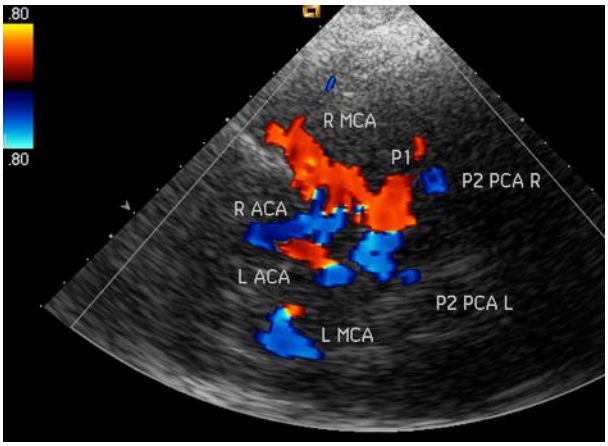

Most importantly, it is used to differentiate vessel occlusion in poor insonation conditions, and to detect very slow blood flow velocities and low flow volumes (small vessels, vessel pseudo-occlusion). Examination of the posterior circulation with contrast agents by insonation through the foramen magnum can increase the depth at which the intracranial vertebral arteries, the basilar artery, and the cerebellar artery segments can be identified and thus improve diagnostic confidence (55, 56).

Technical artifacts may cause inaccuracies:

1. Bolus injection of the contrast agent results in a blooming artifact preventing accurate Doppler spectral measurements. In this situation the setting of the ultrasound device should be adjusted to prevent the confluence of the color signal of adjacent vessels (57).
2. Ultrasound contrast agent injection leads to an artificial increase (1 – 36 %) in maximum blood flow velocity, affecting stratification of a stenosis.

Intracranial stenosis is shown in figures 39 - 43.

Figure 39 60-year-old patient with condition after acute ischemia in the supply area of the left middle cerebral artery. Vascular risk factors: hypertension and nicotine abuse. Sonographic intracranial findings: stenoses of the left middle and left anterior cerebral arteries. Transtemporal insonation on the left with suboptimal visualization of the middle cerebral artery. Arrow = suspected MCA stenosis.

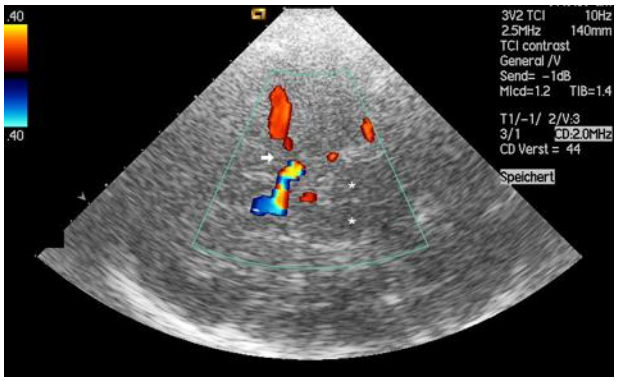

Figure 40 **After application of the echo contrast agent, a blooming artifact appears.**

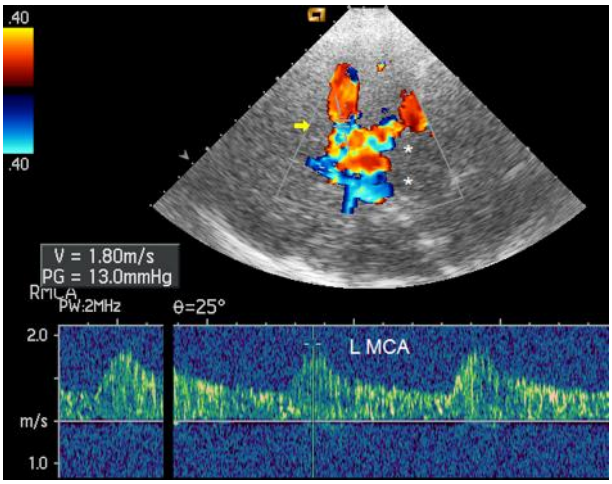

Figure 41 **After the blooming effect has subsided, the stenosis at the origin of the left middle cerebral artery can be better assessed and the Doppler spectrum can be specifically recorded. The maximum systolic flow velocity is 180 cm/s and indicates a moderate stenosis. The bright signals in the Doppler spectrum correspond to the bubbles of the contrast agent. 1 = left middle cerebral artery, *= brainstem, arrow = stenosis of the left middle cerebral artery,**

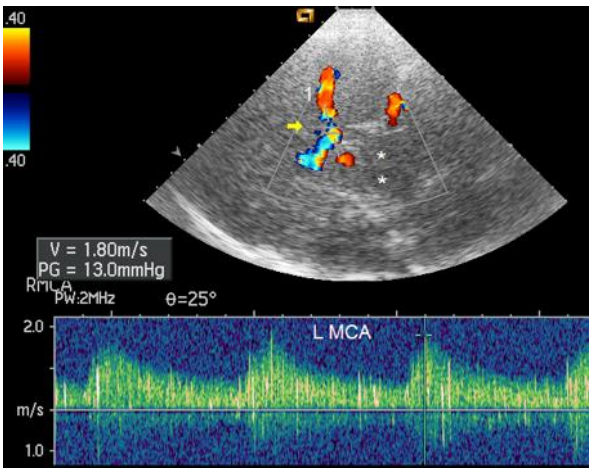

Figure 42 **In the ipsilateral anterior cerebral artery, there are also increased flow velocities (maximum systolic flow velocity = 168 cm/s) with flow disturbances which**

indicate a possible stenosis of the anterior cerebral artery. 1 = left middle cerebral artery, 2 = left anterior cerebral artery (ACA), *= brainstem.

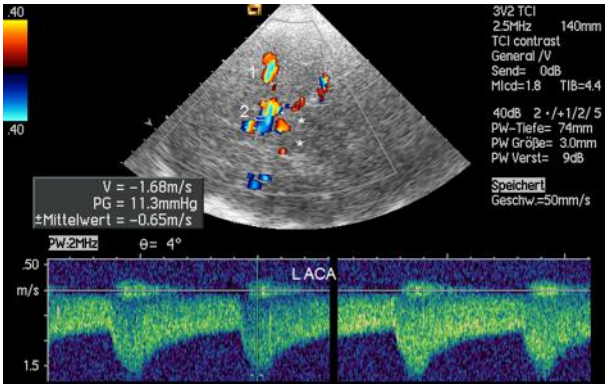

Figure 43 MR angiography confirms the diagnosis of the stenoses of the left middle cerebral artery and the left anterior cerebral artery (arrow). (Diagnostic and Interventional Neuroradiology, University Medicine Göttingen).

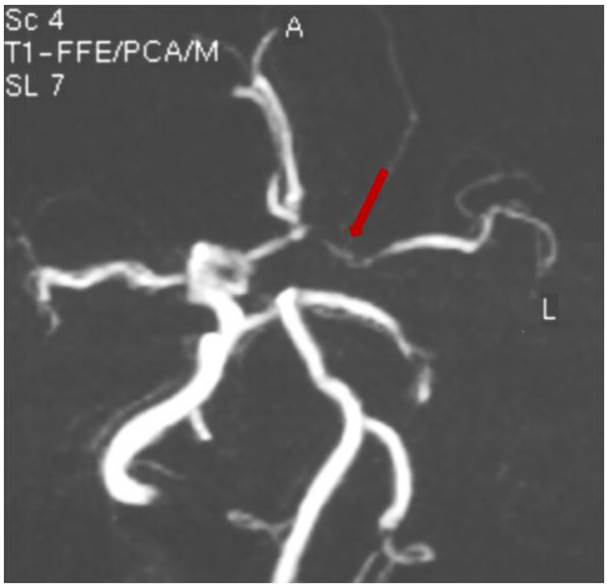

In the event of an ischemic stroke, identifying an intracranial stenosis or vascular occlusion is important for further diagnostics and therapeutic decisions. A diagnosis of occlusion based on the absence of a Doppler signal is not reliable. Use of echo contrast agents helps determine whether the absence of the signal is due to a vascular occlusion or is the result of a technical problem (58). According to the EFSUMB Guidelines and Recommendations, contrast-

enhanced TCD/TCCS improves the diagnostic capabilities of the examination (59). CE-TCCS in intracranial occlusion of the right middle cerebral artery in a 26-year-old man due to a dissection of the extracranial right internal carotid artery is shown in figures 44 - 47.

Figure 44 **Transtemporal examination on the right in the axial plane. The bone window is insufficient, only fragments of the intracranial arteries can be visualized. 1 = Left middle cerebral artery, 2 = Left posterior cerebral artery, 3 = Left anterior cerebral artery, A1 segment, 4 = Anterior cerebral artery, A2 segment, 5 = Right anterior cerebral artery, 6 = Right posterior communicating artery, 7 = Brainstem. The arrow indicates the location of the missing right middle cerebral artery.**

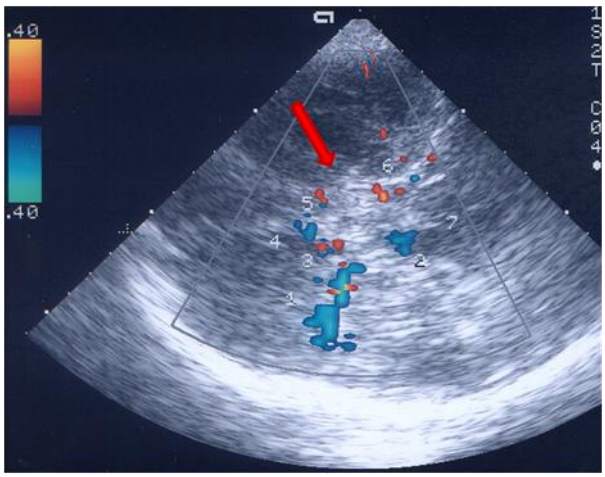

Figure 45 Blooming artifact after application of the contrast agent.

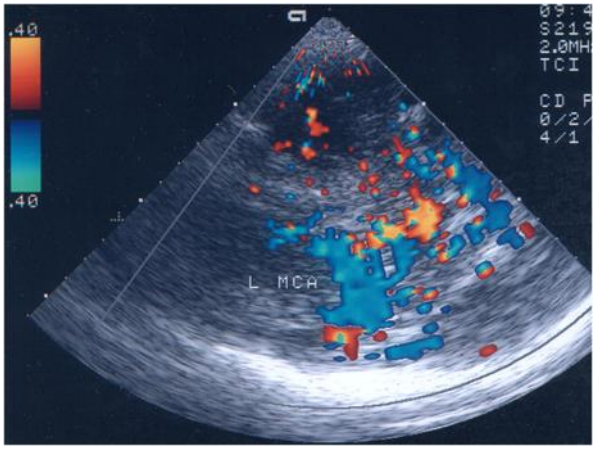

Figure 46 Visualization of the intracranial arteries using the right temporal insonation after the blooming effect subsided. A signal from the occluded right middle cerebral artery cannot be visualized (arrow). The easily visualized ipsilateral posterior cerebral artery is an additional indirect indication of the occlusion of the middle cerebral artery.

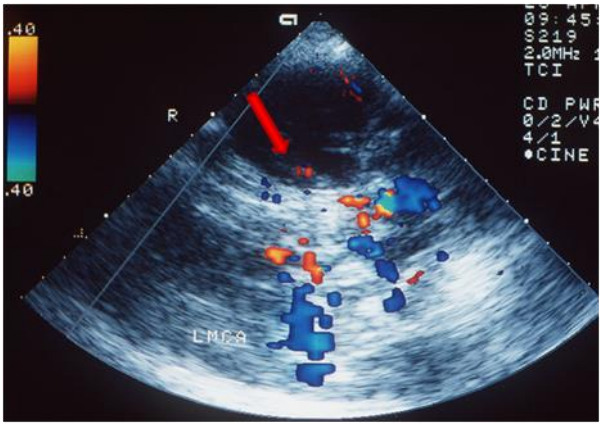

Figure 47 MR-angiogram of the right middle cerebral artery occlusion (arrow). The orientation of the vessels in the picture corresponds to the orientation of the

vessels in the sonographic image. Arrows on MRA image = weak signal of the course of the internal carotid artery.

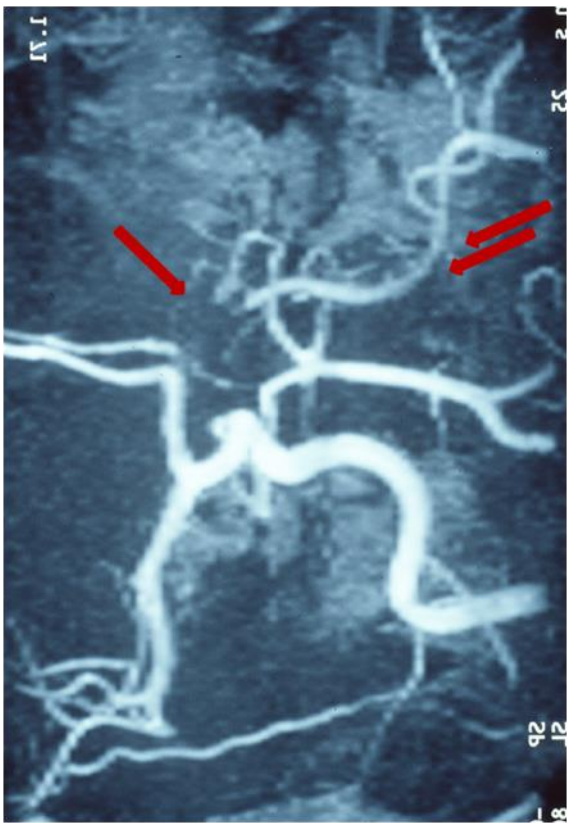

The sonographic evaluation of the **cerebral perfusion** is based on the measurement of blood flow in the microcirculation. Since the beginning of the 1990s, various methods have been introduced and evaluated with regard to clinical application. Harmonic imaging techniques with low mechanical index are mostly used here. SonoVue™, a second-generation ultrasound contrast agent, is suitable for this new imaging modality, because of the specific physical properties of the microbubbles. A specific increase in contrast caused by the harmonic frequencies can be displayed wherever the contrast medium is distributed through the vascular system. It could be shown that the localization and size of an acute ischemia can be visualized on the basis of a corresponding perfusion deficit in the ultrasound examination (60-62). In an own study, stroke patients with malignant space-occupying infarction or cerebral hemorrhage were examined after decompressive craniectomy, to avoid the problems of an unsuitable temporal bone window in transcranial examination. The hypoperfused regions demonstrated by sonography coincided with the respective CT and MRI images (63).

Transcranial contrast imaging of cerebral perfusion following decompressive craniotomy is shown in figures 48 - 50. B-mode sonographic image of cerebral perfusion in a 49-year-old stroke patient after decompressive craniotomy using transcranial B-mode sonography. From: Bartels E., Bittermann H.-J.: Transcranial contrast imaging of cerebral perfusion in stroke patients following decompressive craniectomy. Ultraschall in Med 2004;25:206-213. With permission.

Figure 48 **Transcranial B-mode sonography in the axial diencephalic plane in a 49-year-old patient with a malignant infarction in the territory of the left middle cerebral artery after decompressive craniotomy before (a) and after (b) the application of the contrast agent. The region of the perfusion deficit is hypoechoic in both images (red circle). After the application of the contrast agent, the area of hypoperfusion is clearly delineated.**

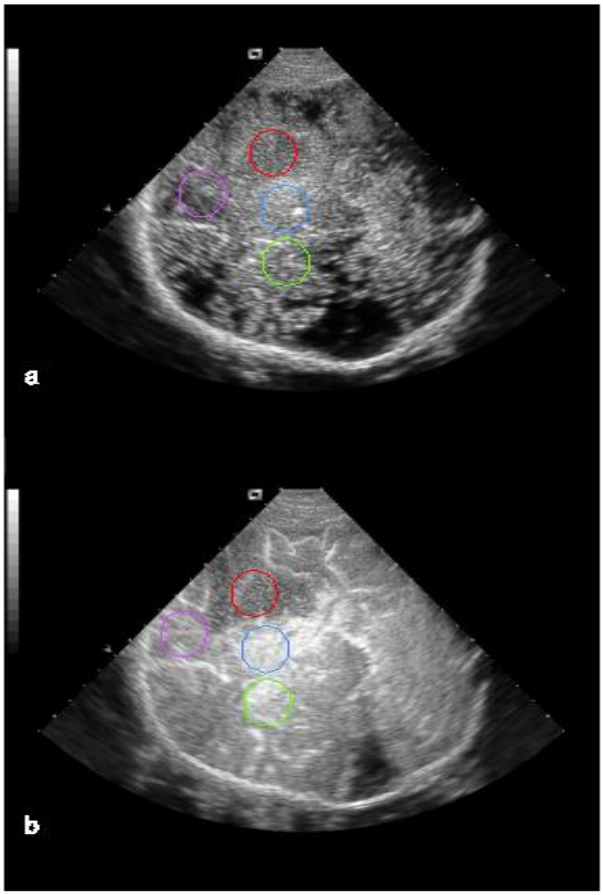

Figure 49 **Time-intensity curves showing the mean intensity values in the area of infarction, in the ipsilateral and contralateral thalamus region and in the ipsilateral frontal lobe. No increase in intensity in the area of infarction (red line) has occured whereas in the ipsilateral thalamus area and in the midline region (blue line) hyperperfusion with a clear increase in intensity appears. Arrow = injection of the contrast agent.**

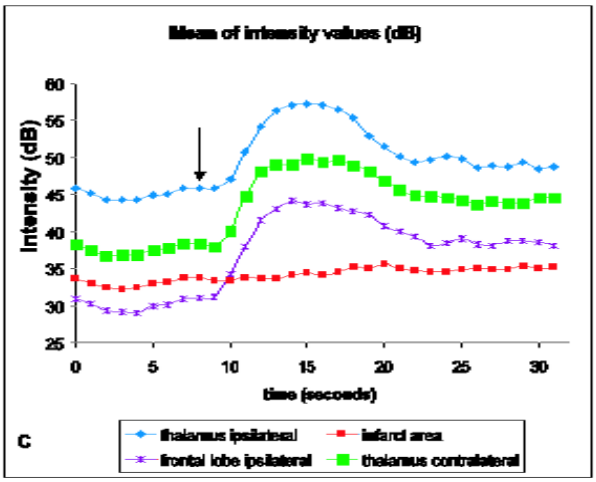

Figure 50 **CT scan showing a malignant infarction in the territory of the left middle cerebral artery after decompressive craniotomy (arrows).**

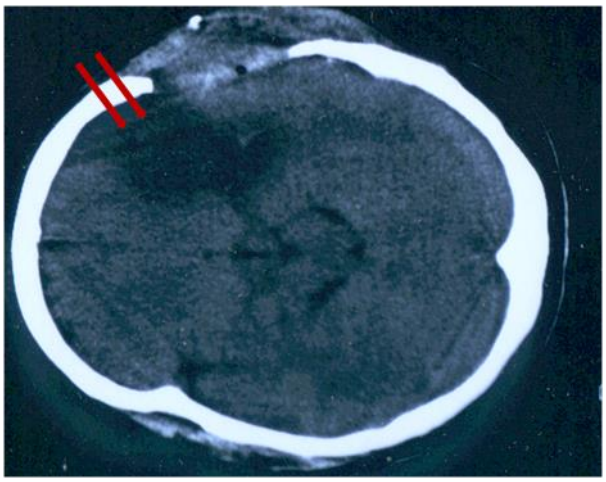

Contrast-enhanced sonography was further optimized by innovative technologies and contrast agent-specific software such as Cadence™ contrast pulse sequencing technology

(CBS, Siemens). Based on our own investigations in stroke patients and in patients with space-occupying intracranial lesions using CPS, a perfusion deficit in the microcirculation of the affected brain area could be visualized, which corresponded well with other cerebral imaging results (64) [Figures 51-52].

Figure 51 **Transcranial contrast imaging of cerebral perfusion using contrast imaging CPS™ technology. Contrast enhanced sonography of the brain parenchyma using Cadence™ contrast pulse sequencing (CPS) technology using the ipsilateral transtemporal insonation in the axial diencephalic plane in a 64-year-old patient with recent ischemia in the left middle cerebral artery territory. A_Visualization of a perfusion deficit in the left middle cerebral artery territory using a triggered registration (time interval 1000 ms, mechanical index MI=1.1). The region of the ipsilateral perfusion deficit is hypoechoic and is marked by a red circle.**

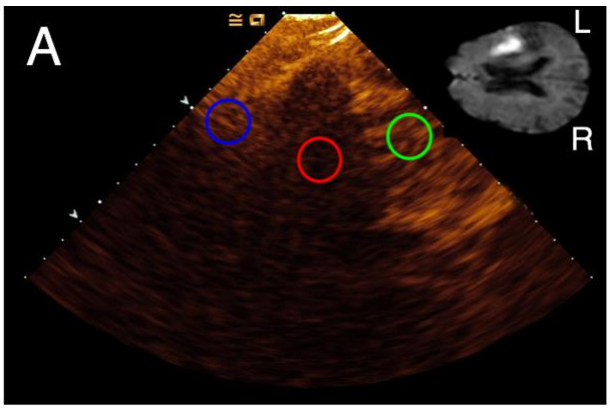

Figure 52 **Time-intensity curves show no increase of intensity in the infarct area (red line). From: Bartels E., Henning S., Wellmer A., Giraldo-Velásquez M., Kermer P.: Evaluation of cerebral perfusion deficit in stroke patients using new transcranial**

contrast imaging CPS™ technology. Preliminary results. Ultraschall in Med 2005;26: 478-486. With permission.

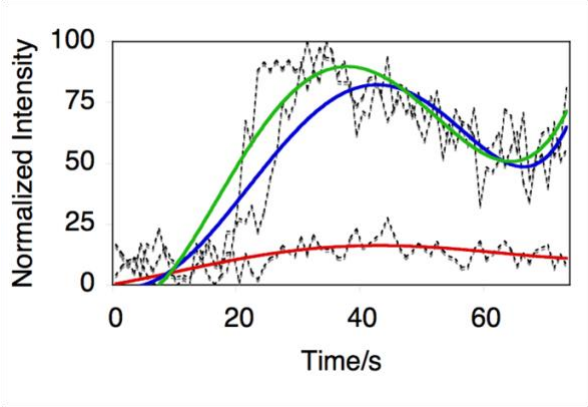

Conclusion

Contrast enhanced ultrasound perfusion imaging has been shown to improve prognostic assessment in the acute phase of cerebral ischemia and to provide comparable results to CT and MR imaging. Disadvantages of the current methods for perfusion display are the dependence on an existing insonation window, the limitation to one examination plain per examination and the real-time evaluation, which is not yet routinely implemented (65, 66).
For this reason, the visualization of cerebral perfusion using contrast-enhanced sonography has not found widespread use in the routine diagnosis of acute stroke. It can be expected that further development in ultrasound technology will also optimize the sonographic examination of cerebral perfusion.

References

1. French LA, Wild JJ, Neal D. The experimental application of ultrasonics to the localization of brain tumors; preliminary report. J Neurosurg 1951;8:198-203.
2. Leksell L. Kirurgisk behandling av skallskador. In: Vortrag: Meeting of Svenska Läkasaällskapet. Stockholm; 1954.
3. Babcock DS, Han BK, LeQuesne GW. B-mode gray scale ultrasound of the head in the newborn and young infant. AJR Am J Roentgenol 1980;134:457-468.

4. Davies P, Stockdale H, Cooke RWI. Ultrasound examination of neonatal heads. Lancet 1979;2:38.
5. Rubin JM, Mirfakhraee M, Duda EE, Dohrmann GJ, Brown F. Intraoperative ultrasound examination of the brain. Radiology 1980;137:831-832.
6. Aaslid R, Markwalder TM, Nornes H. Noninvasive transcranial Doppler ultrasound recording of flow velocity in basal cerebral arteries. J Neurosurg 1982;57:769-774.
7. von Reutern GM. Zerebraler Zirkulationsstillstand Diagnostik mit der Dopplersonographie. Dtsch Arztebl International 1991;88:A-4379-A-4385.
8. Ringelstein EB, Zeumer H, Korbmacher G, Wulfinghoff F. [Transcranial Doppler sonography of the brain-supplying arteries: non-traumatic diagnosis of stenoses and occlusions of the carotid siphon and the middle cerebral artery]. Nervenarzt 1985;56:296-306.
9. Arnolds BJ, von Reutern GM. Transcranial Doppler sonography. Examination technique and normal reference values. Ultrasound Med Biol 1986;12:115-123.
10. Khaffaf N, Karnik R, Winkler WB, Valentin A, Slany J. Embolic stroke by compression maneuver during transcranial Doppler sonography. Stroke 1994;25:1056-1057.
11. Ringelstein EB, Kahlscheuer B, Niggemeyer E, Otis SM. Transcranial Doppler sonography: anatomical landmarks and normal velocity values. Ultrasound Med Biol 1990;16:745-761.
12. Furuhata H. New Evolution of Transcranial Tomography (TCT) and Transcranial Color Dopplar Tomography (TCDT). Neurosonology 1989;2:8-15.
13. Baumgartner RW. Transcranial color duplex sonography in cerebrovascular disease: a systematic review. Cerebrovasc Dis 2003;16:4-13.
14. Bogdahn U, Becker G, Winkler J, Greiner K, Perez J, Meurers B. Transcranial color-coded real-time sonography in adults. Stroke 1990;21:1680-1688.
15. Hashimoto BE, Hattrick CW. New method of adult transcranial Doppler. J Ultrasound Med 1991;10:349-353.
16. Schöning M, Grunert D, Stier B. Transkranielle Duplexsonographie durch den intakten Knochen: Ein neues diagnostisches Verfahren. Ultraschall Med 1989;10:66-71.
17. Bartels E. Farbduplexsonografie der hirnversorgenden Gefässe. In: Color-Coded Duplex Ultrasonography of the Cerebral Vessels/Atlas and Manual; Farbduplexsonografie der hirnversorgenden Gefäße/Atlas und Handbuch. 2. überarbeitete und erweiterte Auflage bilingual, ed. Stuttgart: Schattauer GmbH; 2018.
18. Valdueza JM SSRJ, Klingebiel R. Book: Neurosonology and Neuroimaging of Stroke, Book & DVD. The Neuroradiology Journal 2008;21:594-595.
19. Bartels E, Fuchs HH, Flügel KA. Color Doppler imaging of basal cerebral arteries: normal reference values and clinical applications. Angiology 1995;46:877-884.
20. Bogdahn U, Schlachetzki F. Technical aspects of the clinical examination. In: Echoenhancers and Transcranial Color Duplex Sonography. Blackwell Berlin Blackwell Berlin 1998; 100-111.
21. Bartels E. The axial imaging plane--the main domain of the transcranial color-coded duplex ultrasonography? Eur J Ultrasound 2002;16:47-57.
22. Walter U. Transcranial sonography of the cerebral parenchyma: Update on clinically relevant applications. Perspectives in Medicine 2012;1:334-343.
23. Nedelmann M, Stolz E, Gerriets T, Baumgartner RW, Malferrari G, Seidel G, Kaps M. Consensus recommendations for transcranial color-coded duplex sonography for the

assessment of intracranial arteries in clinical trials on acute stroke. Stroke 2009;40:3238-3244.
24. Bartels E. Transcranial color-coded duplex ultrasonography in routine cerebrovascular diagnostics. Perspectives in Medicine 2012;1:325-330.
25. Baumgartner RW. Transcranial color-coded duplex sonography. Journal of Neurology 1999;246:637-647.
26. Krejza J, Baumgartner R. Clinical Applications of Transcranial Color-Coded Duplex Sonography. Journal of neuroimaging : official journal of the American Society of Neuroimaging 2004;14:215-225.
27. Eggers J, Pade O, Rogge A, Schreiber SJ, Valdueza JM. Transcranial color-coded sonography successfully visualizes all intracranial parts of the internal carotid artery using the combined transtemporal axial and coronal approach. AJNR Am J Neuroradiol 2009;30:1589-1593.
28. Stolz E. Ultrasound examination techniques of extra- and intracranial veins. Perspectives in Medicine 2012;1:366-370.
29. Stolz E, Kaps M, Kern A, Babacan SS, Dorndorf W. Transcranial color-coded duplex sonography of intracranial veins and sinuses in adults. Reference data from 130 volunteers. Stroke 1999;30:1070-1075.
30. Kaps M, Seidel G, Bauer T, Behrmann B. Imaging of the intracranial vertebrobasilar system using color-coded ultrasound. Stroke 1992;23:1577-1582.
31. Schöning M, Walter J. Evaluation of the vertebrobasilar-posterior system by transcranial color duplex sonography in adults. Stroke 1992;23:1280-1286.
32. Becker G, Lindner A, Bogdahn U. Imaging of the vertebrobasilar system by transcranial color-coded real-time sonography. J Ultrasound Med 1993;12:395-401.
33. Bäuerle J, Nedelmann M. B-mode sonography of the optic nerve in neurological disorders with altered intracranial pressure. Perspectives in Medicine 2012;1:404-407.
34. Ertl M, Altmann M, Torka E, Helbig H, Bogdahn U, Gamulescu A, Schlachetzki F. The retrobulbar spot sign in sudden blindness – Sufficient to rule out vasculitis? Perspectives in Medicine 2012;1:408-413.
35. Lovrencic-Huzjan A, Simicevic DS, Popovic IM, Puretic MB, Cvetkovic VV, Gopcevic A, Vucic M, et al. Ultrasonography of the optic nerve sheath in brain death. Perspectives in Medicine 2012;1:414-416.
36. Giller CA. Is angle correction correct? J Neuroimaging 1994;4:51-52.
37. Bartels E, Flügel KA. Quantitative measurements of blood flow velocity in basal cerebral arteries with transcranial duplex color-flow imaging. A comparative study with conventional transcranial Doppler sonography. J Neuroimaging 1994;4:77-81.
38. Martin PJ, Evans DH, Naylor AR. Transcranial color-coded sonography of the basal cerebral circulation. Reference data from 115 volunteers. Stroke 1994;25:390-396.
39. Zipper SG, Stolz E. Clinical application of transcranial colour-coded duplex sonography--a review. Eur J Neurol 2002;9:1-8.
40. Grolimund P, Seiler RW. Age dependence of the flow velocity in the basal cerebral arteries--a transcranial Doppler ultrasound study. Ultrasound Med Biol 1988;14:191-198.
41. Becker G, Lindner A, Hofmann E, Bogdahn U. Contribution of transcranial color-coded real-time sonography to the etiopathogenetic classification of middle cerebral artery stenosis. J Clin Ultrasound 1994;22:471-477.
42. Kaps M, von Reutern GM, Stolz E, von Büdingen HJ. Sonografie in der Neurologie. Stuttgart: Thieme, 2016.

43. Hass WK, Fields WS, North RR, Kricheff II, Chase NE, Bauer RB. Joint Study of Extracranial Arterial Occlusion: II. Arteriography, Techniques, Sites, and Complications. JAMA 1968;203:961-968.
44. Baracchini C, Niederkorn K: Intracranial stenosis/occlusion. In: Baracchini C, Csiba L, eds. Manual of Neurosonology. Cambridge: Cambridge University Press, 2016; 154-164.
45. Baumgartner RW, Mattle HP, Schroth G. Assessment of >/=50% and <50% intracranial stenoses by transcranial color-coded duplex sonography. Stroke 1999;30:87-92.
46. Hoksbergen AW, Legemate DA, Ubbink DT, Jacobs MJ. Collateral variations in circle of willis in atherosclerotic population assessed by means of transcranial color-coded duplex ultrasonography. Stroke 2000;31:1656-1660.
47. Riggs HE, Rupp C. Variation in form of circle of Willis. The relation of the variations to collateral circulation: anatomic analysis. Arch Neurol 1963;8:8-14.
48. Baumgartner RW, Baumgartner I, Mattle HP, Schroth G. Transcranial color-coded duplex sonography in the evaluation of collateral flow through the circle of Willis. AJNR Am J Neuroradiol 1997;18:127-133.
49. Liebeskind DS, Cotsonis GA, Saver JL, Lynn MJ, Turan TN, Cloft HJ, Chimowitz MI. Collaterals dramatically alter stroke risk in intracranial atherosclerosis. Ann Neurol 2011;69:963-974.
50. Becker GM, Winkler J, Hoffmann E, Bogdahn U. Imaging of cerebral arterio-venous malformations by transcranial colour-coded real-time sonography. Neuroradiology 1990;32:280-288.
51. Bartels E. Evaluation of arteriovenous malformations (AVMs) with transcranial color-coded duplex sonography: does the location of an AVM influence its sonographic detection? J Ultrasound Med 2005;24:1511-1517.
52. Klötzsch C, Bozzato A, Lammers G, Mull M, Lennartz B, Noth J. Three-Dimensional Transcranial Color-Coded Sonography of Cerebral Aneurysms. Stroke 1999;30:2285-2290.
53. Bartels E. Aneurysms and arteriovenous malformations (AVMs). In: Echoenhancers and Transcranial Color Coded Sonography. Blackwell Berlin: Blackwell Berlin, 1998; 276 - 297.
54. Droste DW, Boehm T, Ritter MA, Dittrich R, Ringelstein EB. Benefit of echocontrast-enhanced transcranial arterial color-coded duplex ultrasound. Cerebrovasc Dis 2005;20:332-336.
55. Droste DW, Jürgens R, Weber S, Tietje R, Ringelstein EB. Benefit of Echocontrast-Enhanced Transcranial Color-Coded Duplex Ultrasound in the Assessment of Intracranial Collateral Pathways. Stroke 2000;31:920-923.
56. Seidel G, Kaps M. Harmonic Imaging of the Vertebrobasilar System. Stroke 1997;28:1610-1613.
57. Forsberg F, Liu JB, Burns PN, Merton DA, Goldberg BB. Artifacts in ultrasonic contrast agent studies. J Ultrasound Med 1994;13:357-365.
58. Postert T, Braun B, Meves S, Köster O, Przuntek H, Weber S, Büttner T. Contrast-enhanced transcranial color-coded sonography in acute hemispheric brain infarction. Stroke 1999;30:1819-1826.
59. Sidhu PS, Cantisani V, Dietrich CF, Gilja OH, Saftoiu A, Bartels E, Bertolotto M, et al. The EFSUMB Guidelines and Recommendations for the Clinical Practice of Contrast-Enhanced Ultrasound (CEUS) in Non-Hepatic Applications: Update 2017 (Long Version). Ultraschall Med 2018;39:e2-e44.
60. Krogias C, Henneböhl C, Geier B, Hansen C, Hummel T, Meves S, Lukas C, et al. Transcranial ultrasound perfusion imaging and perfusion-MRI--a pilot study on the

evaluation of cerebral perfusion in severe carotid artery stenosis. Ultrasound Med Biol 2010;36:1973-1980.
61. Krogias C, Meves SH, Hansen C, Mönnings P, Eyding J. Ultrasound perfusion imaging of the brain-routine and novel applications: uncommon cases and review of the literature. J Neuroimaging 2011;21:255-258.
62. Seidel G, Cangür H, Meyer-Wiethe K, Renault G, Herment A, Schindler A, Kier C. On the ability of ultrasound parametric perfusion imaging to predict the area of infarction in acute ischemic stroke. Ultraschall Med 2006;27:543-548.
63. Bartels E, Bittermann HJ. Transcranial contrast imaging of cerebral perfusion in patients with space-occupying intracranial lesions. J Ultrasound Med 2006;25:499-507.
64. Bartels E, Henning S, Wellmer A, Giraldo-Velásquez M, Kermer P. Evaluation of cerebral perfusion deficit in stroke patients using new transcranial contrast imaging CPS technology--preliminary results. Ultraschall Med 2005;26:478-486.
65. Eyding J, Krogias C, Schöllhammer M, Eyding D, Wilkening W, Meves S, Schröder A, et al. Contrast-enhanced ultrasonic parametric perfusion imaging detects dysfunctional tissue at risk in acute MCA stroke. J Cereb Blood Flow Metab 2006;26:576-582.
66. Seidel G, Meairs S. Ultrasound contrast agents in ischemic stroke. Cerebrovasc Dis 2009;27 Suppl 2:25-39.